Arab J Geosci (2013) 6:529–541
DOI 10.1007/s12517-011-0379-3

ORIGINAL PAPER

Seismicity associated with active, new-born, and re-awakening basaltic volcanoes: case review and the possible scenarios for the Harraat volcanic provinces, Saudi Arabia

Vyacheslav M. Zobin · Abdullah M. Al-Amri · Mohammed Fnais

Received: 6 June 2011 / Accepted: 8 August 2011 / Published online: 20 August 2011

Abstract During April–June 2009, a swarm of more than 30,000 earthquakes struck the Harrat Lunayyir, situated in the north-western end of the Saudi Arabian Harraat, east of the Red Sea. This sharp increase in the seismic activity in the region of ancient basaltic volcanic centers indicated a likelihood of a future eruption. To check the situation, a short review of the best-documented seismic activity associated with active, new-born, and re-awakening basaltic volcanoes is presented in this article. Basing on the review, some regularity in the development of seismic activity associated with basaltic eruptions was formulated. Three stages in the development of seismic activity were identified: preliminary, preceding, and continuous. The duration of preceding stage varies from a few hours for active and re-awakened volcanoes to some weeks for new-born volcanoes and may serve as a criterion for discriminations of different types of basaltic eruptions. The duration of the seismic activity during the 2009 episode at Harrat Lunayyir was longer than any activity preceding the basaltic eruptions of different types. Therefore, the most probable scenario is the arrest of sub-surface intrusion without any eruption in the region of Harrat Lunayyir. The next probable scenario would be the dike injections along the rift zones. The re-awakening of the old Harrat Lunayyir volcano or the birth of a new volcano at Harrat Lunayyir is less probable.

V. M. Zobin (✉)
Observatorio Vulcanológico de la Universidad de Colima,
Colima, México
e-mail: vzobin@ucol.mx

A. M. Al-Amri · M. Fnais
Department of Geology, King Saud University,
Riyadh, Saudi Arabia

Keywords Basaltic volcano · Earthquake swarm · Harrat Lunayyir · Re-awakening volcano · New-born volcano · Saudi Arabia · Volcanic earthquakes

Introduction

Basaltic lava fields (Harraat) of Arabian Peninsula are characterized by high eruptive potential. Harrigan (2006) reported that during the last 4,500 years, 13 large eruptions occurred within these lava fields. Global Volcanism Program of Smithsonian Institution (GVP 2011) listed six historical eruptions in Arabian Peninsula, three of them in Yemen and three in Saudi Arabia. The most recent eruption of Harras of Dhamar volcano in the north of Yemen occurred in 1937. In the territory of Saudi Arabia, the last eruption, throwing up six cinders cones along a massive fissure south-east of Madinah (Harrat Rahat, Fig. 1), was recorded in the beginning of June 1256. The 0.5 km^3 lava flows reached 23 km distance. The eruption was preceded by earthquake swarm; the strongest of earthquakes were felt in Madinah during a few days before the eruption. The eruption began when the seismic events became more frequent and more intense (Harrigan 2006).

During April–June 2009, a swarm of more than 30,000 earthquakes struck the Harrat Lunayyir (Fig. 1), situated in the north-western end of the Saudi Arabian Harraat, east of the Red Sea. The seismic swarm began on 18 April 2009 (Al-Amri and Al-Mogren 2011). The joint KSU and KACST seismic network, consisting of 21 seismic stations, was installed soon around the volcano, and 398 earthquakes with $mb>3$ were located from 29 April to 27 June 2009, mainly from 1 to 21 May. Two epicentral areas were formed to north and south from Harrat Lunayyir, leaving a free

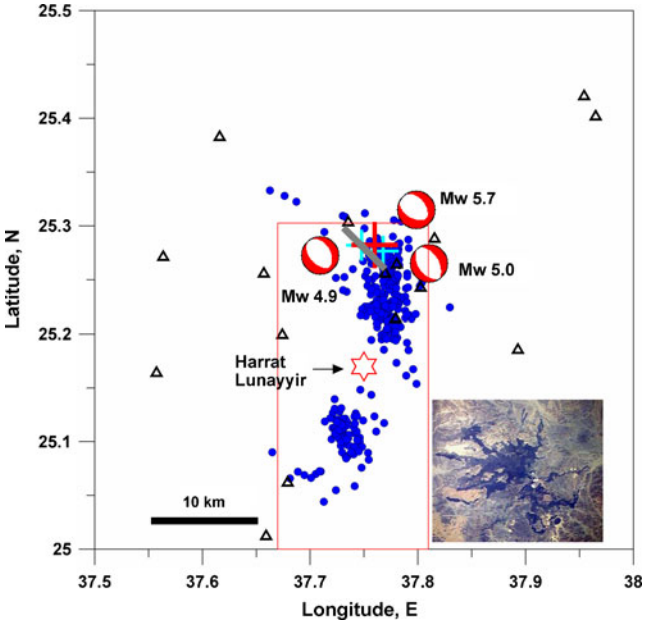

Fig. 1 Epicenters of earthquakes with *mb*>3.0 located by the joint KSU and KACST seismic network at Harrat Lunayyir volcano, Saudi Arabia, during April–June 2009. *Star* shows the volcano; *filled circles* show the earthquake epicenters. The epicenters of three large earthquakes with Harvard CMT solutions are shown with *crosses*; the *largest cross* indicates the position of the largest earthquake with magnitude *Mw* 5.7. The seismic stations are shown with *triangles*. The events presented in cross-section (Fig. 2b) are included within the *red rectangle*. The position of surface ruptures (according to Pallister et al. 2010) is shown with a *broad line*. *Inset* shows the satellite photo of Harrat Lunayyir (NASA Space Shuttle image STS26-41-61, 1988, http://eol.jsc.nasa.gov/). The catalog of earthquakes was taken from Al-Amri and Al-Mogren (2011)

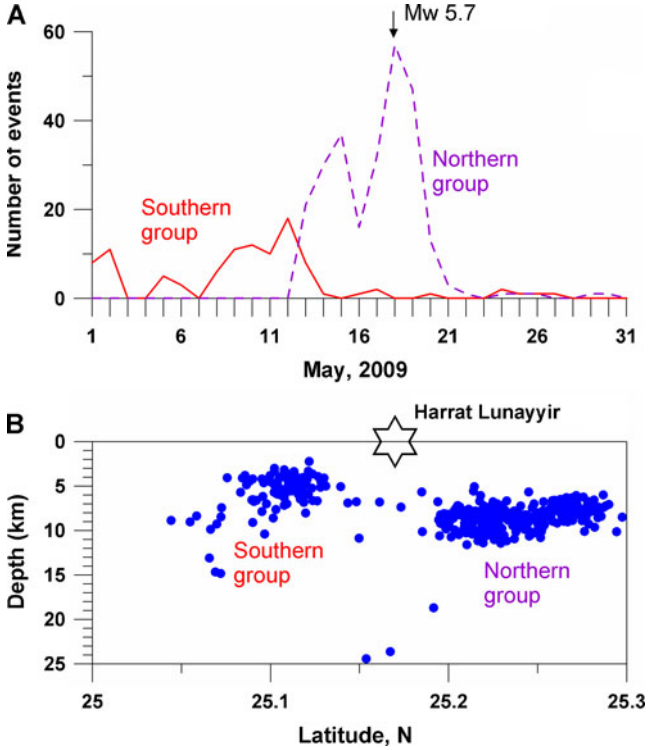

Fig. 2 Temporal development (**a**) and the meridional cross-section of earthquake swarm at Harrat Lunayyir (**b**). In **a**, the *solid line* shows variations in the number of the southern group of events and the *broken line* shows the variations in the number of the northern group of events. *Star* shows the volcano. The catalog of earthquakes was taken from Al-Amri and Al-Mogren (2011)

space beneath the volcano (Fig. 1). During the period from 29 April to 12 May, seismicity developed to south from the volcano. Three earthquakes at the depth between 13 and 15 km were recorded in the very beginning of this sequence on 30 April and 1 May, and then the events clustered within the depth range between 2 and 7 km (Fig. 2). Earthquake frequency reached its maximum on 12 May and then sharply ceased. Maximum magnitude of earthquake was *mb* 3.7.

Beginning from 12 May, the seismic activity was recorded to north from the volcano with a significant increase in the number and magnitude of earthquakes. The seismic activity reached its peak on 19 May. A total of 12 earthquakes with *mb*≥4.0 (USGS 2011) were recorded this day, including the *Mw* 5.7 event. These seismic events clustered at depth between 6 and 11 km, deeper than the initial southern group of earthquakes (Fig. 2).

A north-west trending 8-km-long surface fault rupture with 91 cm of offset was formed (Pallister et al. 2010) near the epicenter of the *Mw* 5.7 earthquake (Fig. 1). The focal mechanism solutions published by Harvard University (Harvard CMT 2011) for three events, located during 19 May (Fig. 1), indicated the normal fault rupturing with the fault planes coinciding with the direction of the surface rupture and with the general direction of the surface structures of Harrat Lunayyir volcano (See inset in Fig. 1). INSAR analysis of interferograms acquired for the period 17–28 June (Pallister et al. 2010) showed that the deformation field at the volcano region was best modeled by intrusion of a 10-km long, NW-trending dike, with a top at less than 2 km depth and volume of about 0.13 km^3. No surface intrusion was observed during 2 years after the seismic episode.

Harrat Lunayyir is one of the smallest Holocene lava fields of Saudi Arabia (see Fig. 1 in Pallister et al. 2010), but individual flow lobes radiate long distances from the center of the Harrat, and flows reached the Red Sea in two places. Harrat Lunayyir contains about 50 volcanic cones that were constructed over Precambrian crystalline rocks along a N–S axis. Lava flows are basaltic to basanitic in composition, and the Holocene flows are alkali olivine basalts. One of the cones may have erupted around the tenth century AD or earlier (GVP 2011).

The system of Saudi Arabian lava fields, situated along the western coast of the Arabian Peninsula, is connected with the Main Ethiopian Rift in northeastern Africa. The study of a 3-D *S*-velocity structure around Arabia and East Africa down to 1,400 km depth, performed by Chang and Van der Lee (2011), showed the origin of the Afar mantle plume in the lower mantle beneath southwestern Arabia.

They suggested that this mantle plume may have contributed, along the Afar plume, to the widespread volcanism and uplift in western Arabia. Pallister et al. (2010), based on seismic and deformation analysis, forecasted the likelihood of a future eruption or large earthquake in the region of Harrat Lunayyir province.

In this article, the case review of best-documented seismic activity recorded prior to some volcanic eruptions at active, new-born, and re-awakening basaltic volcanoes and associated with dike injections along rift zones is presented. Basing on this review, the possible scenarios of the eruption in the northwestern Arabian Harraat are proposed.

Some features of active basaltic volcanoes

Basaltic volcanoes have characteristic lava of low viscosity (10–10^3 poises), high temperature (1,000–1,300°C), with small amount of volatiles (0.2–2 wt.%), and high velocity of movement. They are characterized by effusive and explosive type of eruption and produce extensive lava flows (Spera 2000; Vergniolle and Mangan 2000).

The eruptions of basaltic volcanoes may occur from the summit crater of the volcano, but flank or fissure eruptions are very frequent too. Low-viscosity and high-temperature magmas are very mobile and able to form the passageway to the surface along or out of the central conduit of a volcano. These properties of magma constrain the possible seismic reaction to the magma movement. The fracturing of rock during formation of new volcanic vents on the flanks of a volcano or along a new fissure produces volcano-tectonic earthquakes. These earthquakes can be observed also during the movement of magma along the volcanic conduit before the central eruptions. At the same time, the central eruptions of basaltic volcanoes may frequently occur without any preliminary volcano-tectonic activity.

The seismic activity recorded prior to the eruptions of active basaltic volcanoes is rather short (from 1 to 100 h) and occur at shallow depths. For basaltic volcanoes, the most frequent is a preliminary seismic sequence with the maximum number of events in the beginning of the sequence. As usual, the eruption begins during the decrease of seismic activity or when the seismic activity is ceased (Zobin 2003). The examples of seismic activity associated with the summit and lateral eruptions at active basaltic volcanoes are shown below.

Kilauea Volcano, Hawaii

The 1982 summit caldera eruption occurred on 30 April and continued for 1 day. The short swarm of earthquakes began about 2.5 h before the eruption and continued up to the beginning of the volcanic manifestations (Fig. 3).

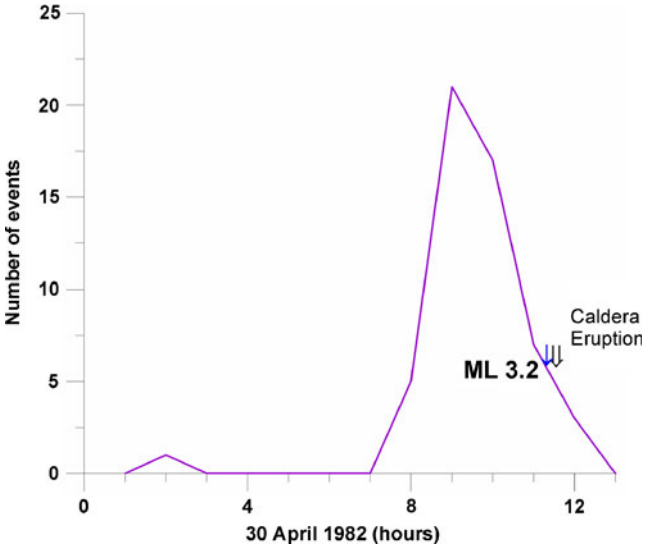

Fig. 3 Temporal variation of earthquakes before the 30 April 1982 Kilauea eruption. A *single arrow* indicates the moment of maximum earthquake; the *double arrow* indicates the beginning of magma intrusion. Data are from the catalog of Hawaiian Volcano Observatory

The majority of earthquakes were recorded during the first hour of activity; then the number of events gradually decreased. The maximum magnitude event (ML 3.2) was recorded just before the beginning of the eruption.

The epicenters of all 47 events recording between 08:54 and 11:41 were located within the summit caldera, where the eruptive fissures opened (Fig. 4a). Earthquake depths were estimated within the range from 1 to 3 km beneath the caldera (Fig. 4b).

Mount Etna, Sicily

The lateral eruption of 17 July 2001 at Mount Etna volcano occurred along the 6-km-long sub-meridional system of fissures that were opened on the southern side of the south-east summit crater (SEC) at about 3,000 m a.s.l. (Fig. 5). It lasted for 24 days and produced a total of 25×10^6 m^3 of lava. In addition, about 5×10^6 m^3 of tephra were emitted, making this an unusually explosive lateral eruption. The eruption occurred on background of the sequence of 15 Strombolian bursts occurring from 7 June to 17 July (Alparone et al. 2004; Allard et al. 2006).

Figure 6 shows the temporal variations in volcano-tectonic activity during June–July 2001 recorded by the seismic network of the National Institute of Geophysics and Volcanology, Section Catania (Patanè et al. 2003). The threshold of the catalog is $Md\geq1.5$. The epi- and hypocenters of these seismic events are shown in Fig. 5. It is seen that during the Strombolian bursts activity the daily number of volcano-tectonic earthquakes was between 0 and 7. Seismic activity sharply increased on 12 July reaching 173 events on 13 July, one of them was the largest of the

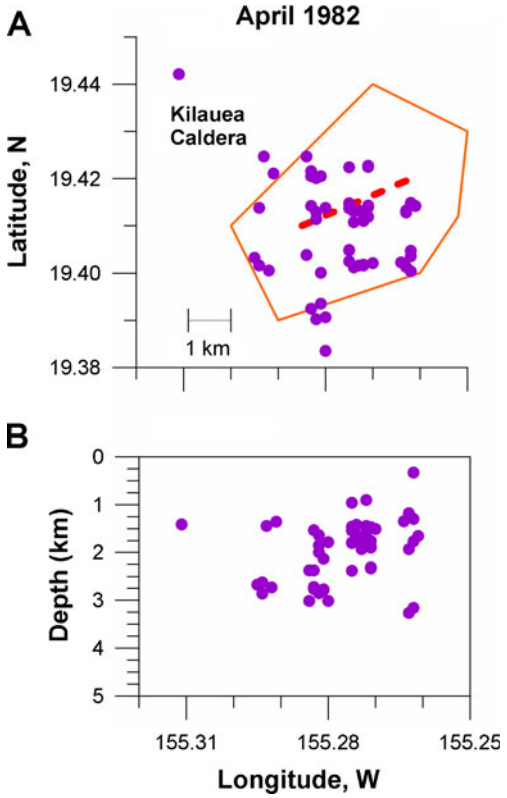

Fig. 4 Epicenters (**a**) and hypocenters (**b**) of earthquakes associated with the 30 April 1982 summit caldera eruption at Kilauea volcano, Hawaii. The outline of the caldera (*solid lines*) and the new eruptive fissure (*dashed lines*) are shown according to Klein et al. (1987). Data are from the catalog of Hawaiian Volcano Observatory

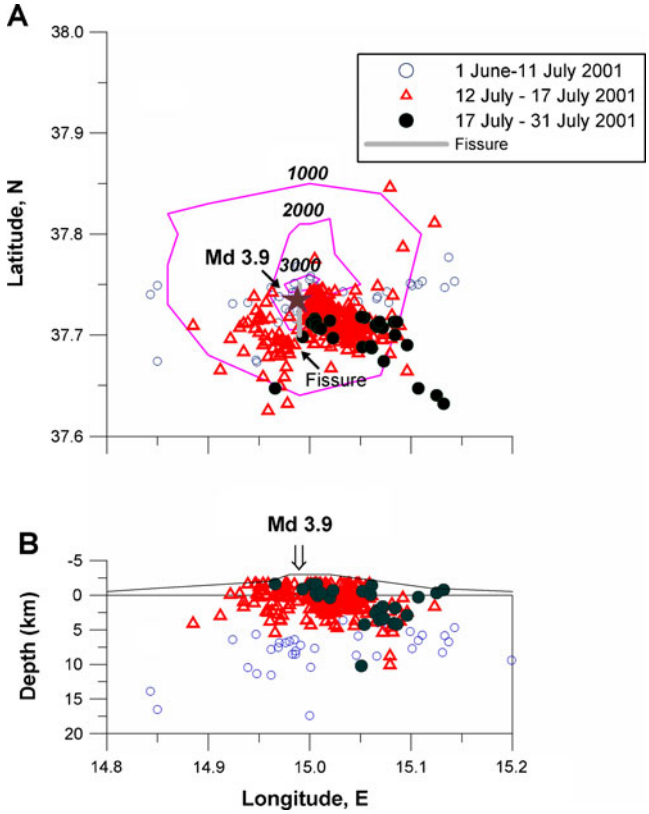

Fig. 5 Epicenters (**a**) and hypocenters (**b**) of the earthquakes associated with the 2001 lateral eruption of Mt. Etna. The largest earthquake (*Md* 3.9) epicenter is shown in (**a**) with the *star*. Its projection is shown also in (**b**) with the *arrow*. The fissure zone is shown according to Alparone et al. (2004). Earthquake data are from the catalog of the National Institute of Geophysics and Volcanology, Section Catania

seismic swarm events with magnitude *Md* 3.9 (it occurred in 5 h after the beginning of the swarm; Fig. 6). The total seismic activity continued for about 120 h. During 14 to 18 July, the number of earthquakes gradually decreased, and the lateral eruption began on 17 July from six eruptive fissures, accompanied by strong explosive activity and destructive lava flows. After the beginning of eruption and till the end of eruption on 9 August, daily seismicity stayed at low level (0–2 daily events with magnitude $Md \geq 1.5$).

Seismicity associated with the background Strombolian activity, recorded from 7 June to 17 July, was located along the broad ENE–WSW zone going through the summits of Etna and distributed at the depth range from 5 to 20 km b.s.l. (Fig. 5). The preliminary 12–17 July swarms of volcano-tectonic earthquakes clustered into two compact groups of events, western and eastern, separated by sub-meridional fissure zone. The foci of both groups of events were distributed at the depths from 5 km b.s.l to 2 km a.s.l, mainly within the volcanic edifice. The largest *Md* 3.9 earthquake was located between these two groups of earthquakes within the fissure zone, at the depth of the sea level. The earthquakes, recorded during the lateral eruption at the depths from 5 km b.s.l to 2 km a.s.l., were

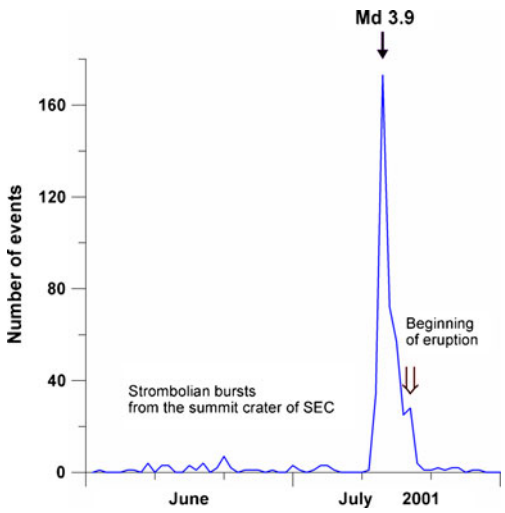

Fig. 6 Temporal variations of the earthquakes associated with the 2001 lateral eruption of Mt. Etna. The *arrow* shows the onset of the largest earthquake (*Md* 3.9) of the swarm and the *double arrow* shows the beginning of eruption. Data are from the catalog of the National Institute of Geophysics and Volcanology, Section Catania

located within the eastern cluster and on its continuation in SSE direction. No visible fissures were reported for this direction but may be they were formed at the depths without opening on the surface.

Seismic activity associated with new-born basaltic volcanoes

New-born basaltic volcanoes are usually monogenic. They may be formed within the continental rift zones and during the submarine volcanic activity. The most famous examples of the continental new-born volcanoes are Parícutin (1943) and Jorullo (1759) volcanoes within the Michoacán-Guanajuato volcanic field, México (Luhr and Simkin 1993); New Tolbachik volcanoes (1975) within the Tolbachik Dol, Kamchatka (Fedotov 1984); and Huoshaoshan volcano (1720) within the Wudalanchi volcanic group, China (Chen et al. 2004). Between new submarine volcanic centers may be referred to Teishi Knoll volcano (1989) within the Izu volcanic group, Japan (Yamasato et al. 1991) and CoAxial Segment volcano (1993) within Juan de Fuca submarine ridge (Dziak et al. 1995). All these eruptions were preceded by shallow seismic activity. The best-documented seismological examples are the 1975 eruption of New Tolbachik volcanoes and the 1989 Teishi Knoll eruption.

New Tolbachik volcanoes, Kamchatka, Russia

A chain of new volcanoes was formed from 6 July 1975 to 10 December 1976 along the 12-km-long fissure that was opened within the Tolbachinsky Dol of Holocene cinder cones about 18 km SW from active basaltic Plosky Tolbachik volcano (Fig. 7). Eight new volcanoes were basaltic cinder cones with a height up to 300 m; 1.2 km^3 of lava was produced by the cones, which covered an area of about 45 km^2. The total volume of pyroclastic material was about 1 km^3 (Fedotov 1984).

The preceding swarm of earthquakes began on June 27 (Zobin and Gorelchik 1982). It is possible to discriminate two stages in the seismic activity (Fig. 8): from 27 June to 30 June and from 1 July to 5 July. During the first stage, a sharp increase in the number of events was observed on 27 June, and then the number gradually decreased for 3 days. The epicenters were distributed within an ellipse-shaped area just to the north from the site of forthcoming eruption of the cone I (Fig. 7a) and covered the space where the following seven cones appeared. The depths of earthquakes varied from 15 km to the surface (Fig. 7b).

The second impulse in seismic activity was characterized by lower number of events and ceased 1 day before the July 6 eruption. The epicenters occupied more compact area

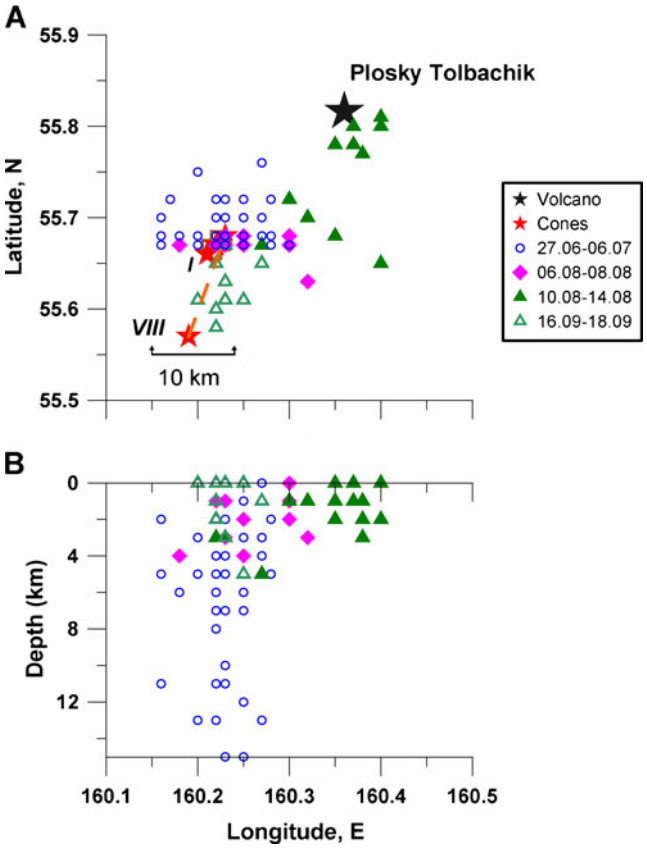

Fig. 7 Epicenters (**a**) and hypocenters (**b**) of earthquakes (*mb*>2) that were observed during the June–September 1975, forming of eight new Tolbachik volcanoes. Four groups of events are shown: 26 June–6 July (*crosses*); 6–8 August (*diamonds*); 10–14 August (*black triangles*), and 16–18 September (*open triangles*). Cones I to VIII are shown by *gray stars*; active volcano Plosky Tolbachik is shown by *black star*. The fissure zone is shown by *dashed line*. Data are from the Kamchatka Regional Earthquake Catalog

than during the first stage, nearer to the forthcoming eruption site. They were shallower and were distributed from 8 km of depth to the surface. Two largest earthquakes of the swarm (*Mw* 4.9) were observed during the second stage, on July 2 at the depth of 11 km. Their epicenters were located below the site of forthcoming cones II and III.

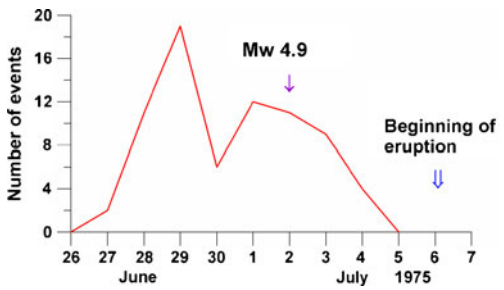

Fig. 8 Temporal variations of daily number of earthquakes (*mb*>2) preceding the 6 July 1975 eruption of the first cone of New Tolbachik volcanoes. The moment of largest event is shown. Data are from the Kamchatka Regional Earthquake Catalog

During the following eruptive activity with the formation of new cones in August–September, 1975, a few seismic sequences were observed (Fig. 7). One sequence (11 events with $mb>2$) occurred from 6 to 8 of August and preceded the birth of cone II on 9 August. The epicenters were distributed within the southern part of epicentral zone of the first swarm of 26 June–6 July, on the level of the forthcoming site of cone II. The next sequence of small earthquakes (35 events with $mb>2$) occurred from 10 to 14 August, before the forming of the third and fourth cones on 17 August. These seismic events connected the new eruptive zone with the old basaltic Plosky Tolbachik volcano (Fig. 7a).

The last seismic swarm (12 events with magnitude $mb>2$) was recorded from 16 to 18 September 1975, preceding the birth of cone VIII (Fig. 7). The location of these events continued the active line from Plosky Tolbachik volcano through the North Zone of cones I–VII (they finished their activity on 15 September) to the south up to the site of cone VIII that was born on 18 September.

Teishi Knoll Volcano, Izu Islands, Japan

On 30 June 1989, an earthquake swarm started off eastern Izu Peninsula in Japan (Fig. 9). This was then culminated by the submarine eruption on 13 July. The hourly numbers of earthquakes (Fig. 10) that were observed at station KMT, situated at a distance of 6.8 km from the eruption site (Fig. 9), show that three main stages in development of the swarm were observed: (1) from 30 June to 4 July; (2) from 4 July to 8 July, and (3) from 8 July to 13 July (Yamasato et al. 1991).

During the stage 1 seismic activity was very low; the great increase in the number of events began from 4 July, and then gradually decreased during the next 3 days (stage 2). The next large impulse in seismic activity (stage 3) began on 8 July and reached its maximum on July 9, when the M_{JMA} 5.5 earthquake, largest in this sequence, occurred. Then the seismic activity gradually declined and the eruption began on 13 July with a low background level.

Figure 9 demonstrates that a regularization of the epicentral zone of events during the swarm was observed. During the first and second stages, the epicentral zone had an elliptical form (Fig. 9b). At the third stage, the epicenters clustered in a lineal sub-meridional zone including the site of forthcoming eruption (Fig. 9c and d). After the beginning of the eruption, the seismic events continued to cluster within this lineal zone. The majority of seismic events of the swarm were located within depth range from 5 to 10 km (Fig. 9f). Two hypocentral subzones were formed: the initial large subzone just below the eruption site that was active during stages I and II, and a narrow smaller size subzone that was formed during stage III of the swarm activity. A thin lineal zone of a few events connects the large hypocentral subzone with the site of eruption (Fig. 9f).

Seismic activity associated with dike injections along rift zones

This type of eruption is practically a birth of new volcano center also but without forming of a cinder cone. The 2005 Dabbahu, Ethiopia, rifting episode occurred in the southernmost Red Sea rift near the Afar triple junction. Afar region was affected by seismo-tectonic crisis during 1978 and 1989 (Ayele et al. 2007). Dabbahu is a Holocene volcanic massif forming an axial range of the Afar depression. The obsidian flows, lava domes, and pumice cones form the summit and upper flanks of the volcano, which was built over a base of basaltic-to-trachytic lava flows of a shield volcano. Late-stage Holocene basaltic fissure eruptions occurred at the NW base of the volcano. Abundant fumaroles are located along the crest of the volcano and extend NE. The first historical eruption of Dabbahu volcano took place from 26 to 30 September 2005 from a fissure vent on the NE flank of the volcano. It was a small explosive eruption that produced ash fall deposits. The 2005 event ruptured the length of a magmatic segment within the Dabbahu-Manda Hararo segment of the Manda-Hararo rift zone (BGVN 2005; Ayele et al. 2007; Ebinger et al. 2010).

The seismic crisis began on 4 September 2005 (Ayele et al. 2009). Activity subsided but then restarted on 20 September and continued until 4 October (Ebinger et al. 2010). The 2005 epicentral zone was developed between Ado'Ale Volcanic Complex (AVC) and DVC (Fig. 11). Two impulses of seismic activity were observed: from 20 to 23 September and from 23 to 26 September (Fig. 12). Nine earthquakes with magnitudes Mw between 5.0 and 5.5 (USGS 2011; Harvard CMT 2011) were recorded. The largest Mw 5.5 event occurred on 24 September at the peak activity of the second seismic impulse. The 26 September eruption began when the number of earthquakes decreased (Fig. 12). The September 2005 eruption vent was situated approximately 5 km ENE of the Dabbahu volcano summit (Fig. 11) (Ayele et al. 2007).

Subsequent fissure basalt intrusions, displayed by continuous earthquake swarms (Fig. 11), were recorded during June 2006 to June 2009 along the Dabbahu-Manda Hararo rift segment, in its central and southern parts (Ebinger et al. 2010). The site of the 14 August, 2007 mafic eruption in the Karbahi graben south of AVC (Ayele et al. 2009) is shown in Fig. 11.

Total of 420 earthquake hypocenters, located during 2005–2009 along the 120-km-long rift segment, clustered between 2 and 12 km. The largest of them show rift-normal opening (Ayele et al. 2009; See also Fig. 11). The post-diking earthquakes mimic the geodetically determined distribution of the 2005 dike (Ebinger et al. 2010).

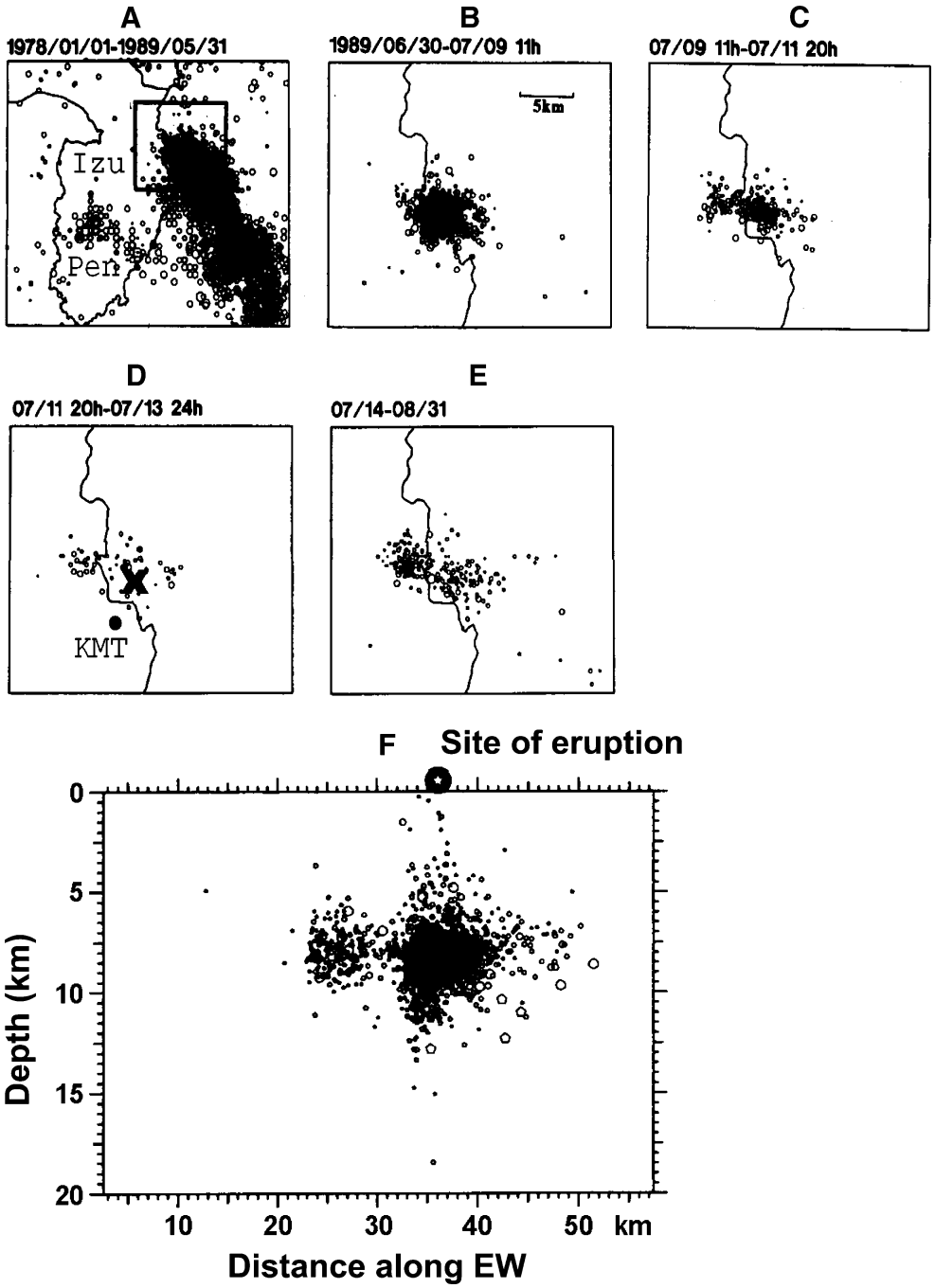

Fig. 9 Spatial-temporal development of the 1989 Teishi-knoll earthquake swarm. **a** Seismic activity of the zone of eruption before the swarm (January 1978-31 May 1989); **b** Seismicity during the first and the second stages of the swarm (30 June – 9 July, 11:00, 1989); **c** Seismicity during the third stage of the swarm (9 July, 11:00 – 11 July, 20:00, 1989); **d** Seismicity just before the eruption (11 July, 20:00 – 13 July, 24:00, 1989); **e** Seismicity during the eruption (14 July – 31 August 1989). **f** Depth distribution of the 1989 Teishi Knoll earthquake swarm events along the EW direction. *Inset* in (**a**) shows the area of study in Figs. B-E. *Cross* in (**d**) shows the site of eruption. KMT is the seismic station. A *black circle* on the surface level in (**f**) shows the site of eruption. Collated from Matsumura et al. (1991) and Yamasato et al. (1991)

Seismic activity associated with re-awakening basaltic volcanoes

An example of re-awakening of basaltic volcano was observed in Kamchatka, Russia when an explosive eruption in Karymskoye lake, situated within the caldera of Academia Nauk volcano, occurred on 2 January 1996. It was the first historic eruption of Academia Nauk volcano after 4,800 years of repose (Belousov and Belousova 2001). Eruption developed with a discharge rate of basaltic magma of about 10^6 kg/s through an initial water depth of ~50 m and its total duration was about 20 h only. By the end of the eruption, the pyroclastic deposits formed a new peninsula in the northern part of the lake (Fedotov 1998).

The Akademia Nauk caldera is crossed by a major NNE regional fault that goes along the volcanic chain and is considered as a deep-seated magma-outletting fault of this volcanic chain (Masurenkov 1991). Rare eruptions of basic magma had occurred along the fault in the late Pleistocene–early Holocene; they built several scoria cones and maars to the north of caldera and also an underwater tuff ring inside the caldera.

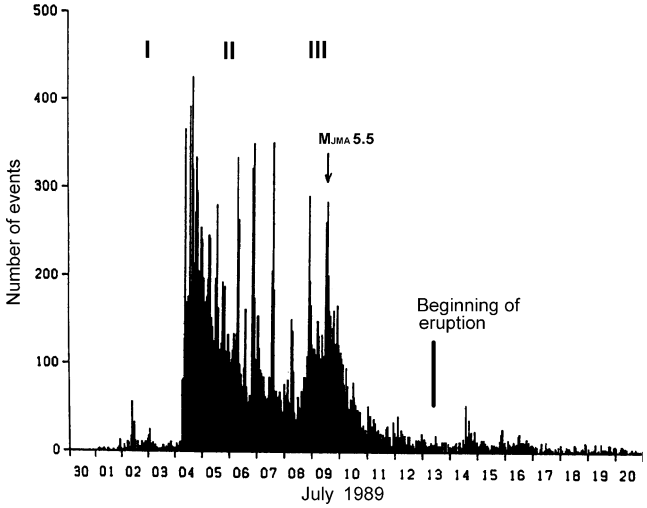

Fig. 10 Temporal variations of the number of earthquakes during the 1989 Teishi Knoll swarm according to data of station KMT (see Fig. 9d). I, II, and III are the stages of the swarm. From Yamasato et al. (1991)

During 24 years before the eruption, the seismic activity developed around Karymskoye lake at depths of 0–22 km, with the majority at depths between 5 and 15 km. The events clustered to the south of neighboring Karymsky volcano along the regional fault (Figs. 13a and 14a). The main preliminary swarms were recorded in 1978, 1992, and 1995. The maximum magnitude of 1972–1995 events was *Ms* 5.5 that was observed during the January 1978 crisis (Zobin et al. 1983).

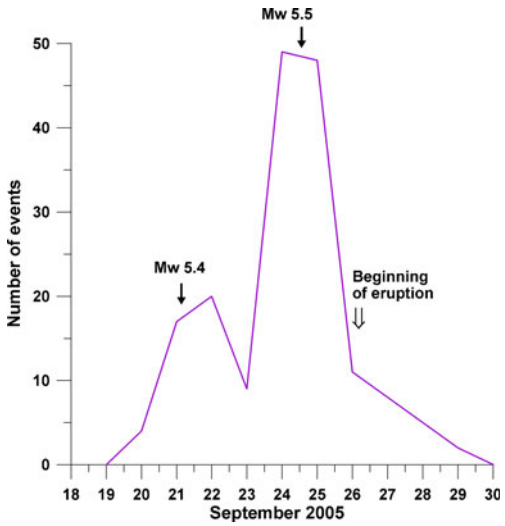

Fig. 11 Temporal distribution of earthquakes before the 26 September 2005 eruption during the Dabbahu rifting episode. Data from the catalog of USGS (2011). *Two single arrows* indicate the moments of maximum earthquakes, their magnitudes *Mw* were taken from (Harvard CMT 2011); the *double arrow* indicates the beginning of magma intrusion

A sharp increase in seismic activity was observed on 1 January 1996 (Fig. 15). The process began with the 2-h sequence of 199 very small (magnitude *mb* about 0) events below the crater of Karymsky volcano and developed up to the site of Karymskoye lake (Fig. 13b). The second sequence included 58 events of magnitude *mb* greater than two. Majority of them occurred at depth between 2 and 20 km; but nine events were recorded between 40 and 60 km (Fig. 14b). This sequence continued for 4 h and was culminated in the *Mw* 7.1 earthquake. The focal mechanism of the large shock (Zobin and Levina 1998) was characterized as a strike-slip along the fault plane coinciding with the strike of the regional fault (Fig. 13b).

The third, aftershock, sequence of seismic events occupied the area of the second sequence epicenters and spread also to the south-west along the regional fault. This sequence consisted of 261 events with magnitudes *mb* greater than 2 and continued for about a month gradually decreasing. The eruption of new volcanic center in the Karymskoye Lake occurred in about 14 h after the beginning of aftershock sequence (Zobin and Levina 1998).

The application of finite-fault, broad-band teleseismic *P* waveform inversion to the *Mw* 7.1 earthquake (Zobin and Levina 1998) demonstrated that the main feature of the rupture process was the breaking of two large asperities at depths from 0 to 12 km and from 20 to 35 km beneath the Karymskoe Lake (Fig. 14). The majority of small earthquakes were located between these two asperities at depths from 12 to 20 km. The position of broken asperities allows suggesting that during the large earthquake rupturing an ancient magmatic column beneath the volcano was destroyed. Small 1972–1995 earthquakes were able only to destroy the intermediate-depth part of the column between 12 and 20 km. The main work for opening a magma passageway to the surface was made by the large *Mw* 7.1 shock that had broken the upper and deep parts of the ancient magmatic column.

The main difference in the seismic activity just before the beginning of the 1996 eruption and the seismic activity of 1972–1995 was in the deeper distribution of the foci of the January 1996 earthquake sequence and in the appearance of large *Mw* 7.1 earthquake.

Results and discussion

Data presented in the previous sections allow us to formulate some regularity in the development of seismic activity associated with basaltic eruptions. Periods of seismic activity may be separated into three stages:

Stage 1 Preliminary. A sequence of seismic swarms without eruptions; may continue for a few years.

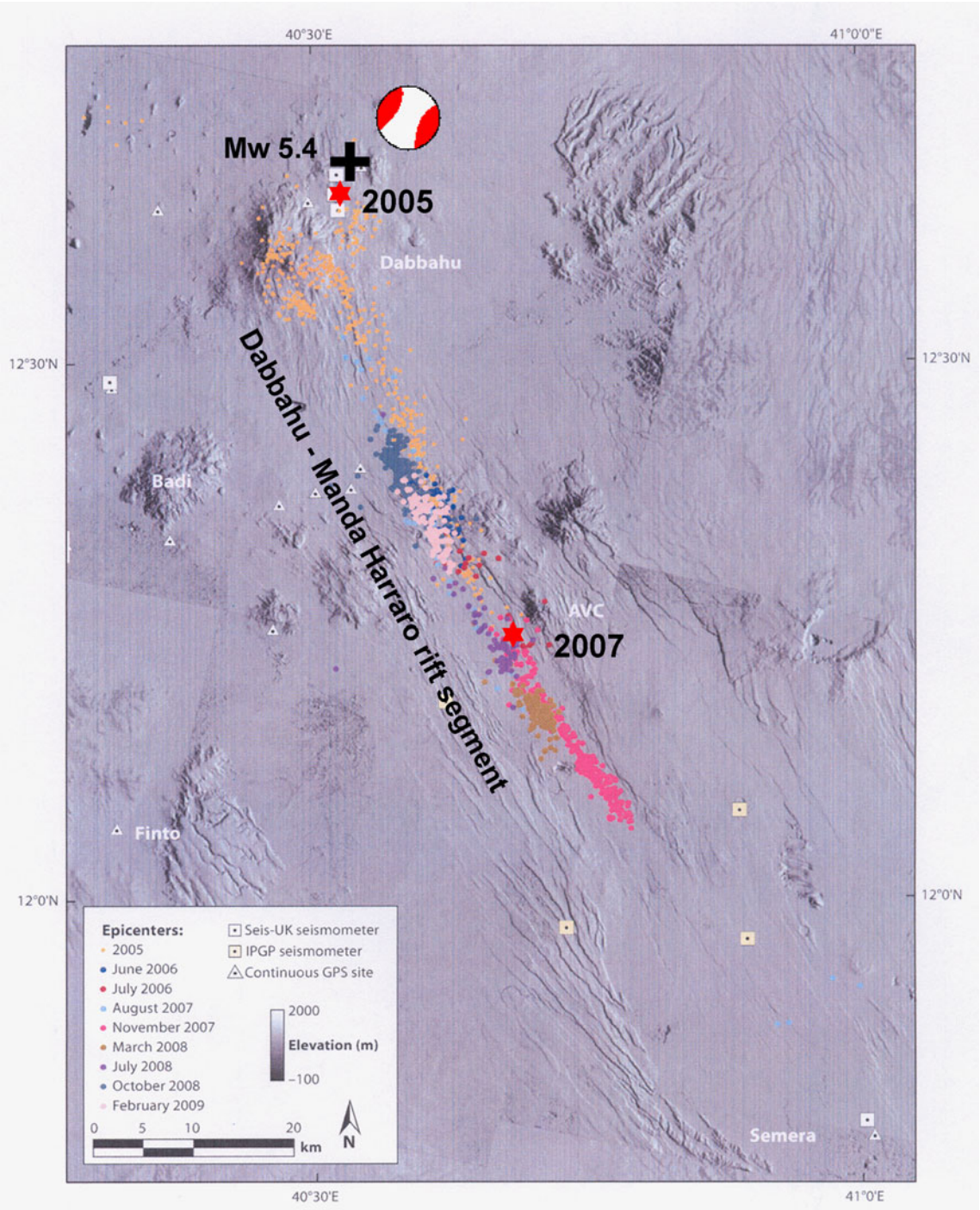

Fig. 12 Epicenters of earthquakes in the Dabbahu-Manda Hararo segment from 19 October 2005 to 2009, with a 6-month gap between October 2006 and March 2007. *Squares* are Seis-UK seismic stations operational in 2005/2006 and IPGP seismometers deployed in 2007; *triangles* are continuous GPS sites. The composite digital elevation model is constructed from Spot 5 imagery; vertical resolution <10 m. Ado'Ale volcanic complex (*AVC*) is a chain of rifted silicic centers at the segment center. Semera is the Afar region's capital. *Stars* show the sites of the 26 September 2005 and the 14 August 2007 eruptions. The ISC epicenters of the largest *Mw* 5.4, 20 September 2005 and *Mw* 5.5, 24 September 2005 earthquakes (ISC 2011) are shown by *crosses*. Their Harvard CMT focal mechanisms (Harvard CMT 2011) are shown. From Ebinger et al. (2010) with modifications

Stage 2 Preceding. Seismic swarms occurring just before the eruption; may continue during time interval from a few hours to a few weeks.

Stage 3 Continuous. A sequence of seismic swarms occurring after the initial eruption with formation of new volcanic centers; may continue for a few years.

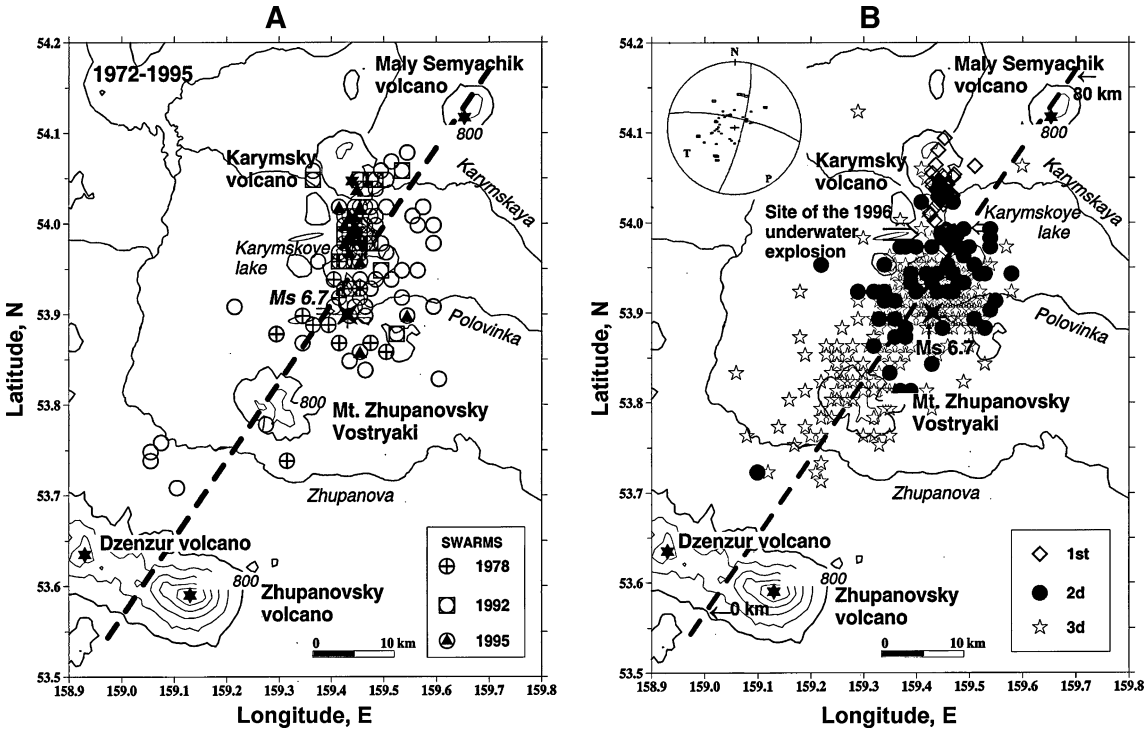

Fig. 13 Epicenters of earthquakes (*mb*>2) located during 1972–1995 (**a**) and in January 1996 before the eruption in Karymskoye lake (**b**). **a** The *open circles* show the epicenters of the earthquakes. The epicenters of the three main swarms of 1978, 1992, and 1995 are noted by special symbols as shown. The volcanoes are shown by the *black stars*; the epicenter of the *Mw* 7.1 event is shown by the *4-pointed star*. The regional fault is shown by *dashed line*. **b** The *1st*, *2nd*, and *3rd* are the symbols for epicenters of three earthquake sequences on dates. Focal mechanism of the *Mw* 7.1 event (Zobin and Levina 1998) is shown in the left corner. Data are from the Kamchatka Regional Earthquake Catalog

Table 1 shows the presence of these stages (or part of them) for different types of eruptions. Stage 2 is characterized by a variable duration for different type of eruptions (Fig. 16). The duration of this stage varies from a few hours for active and re-awakened volcanoes to some weeks for new-born volcanoes and may serve as a criterion for discriminations of different types of basaltic eruptions.

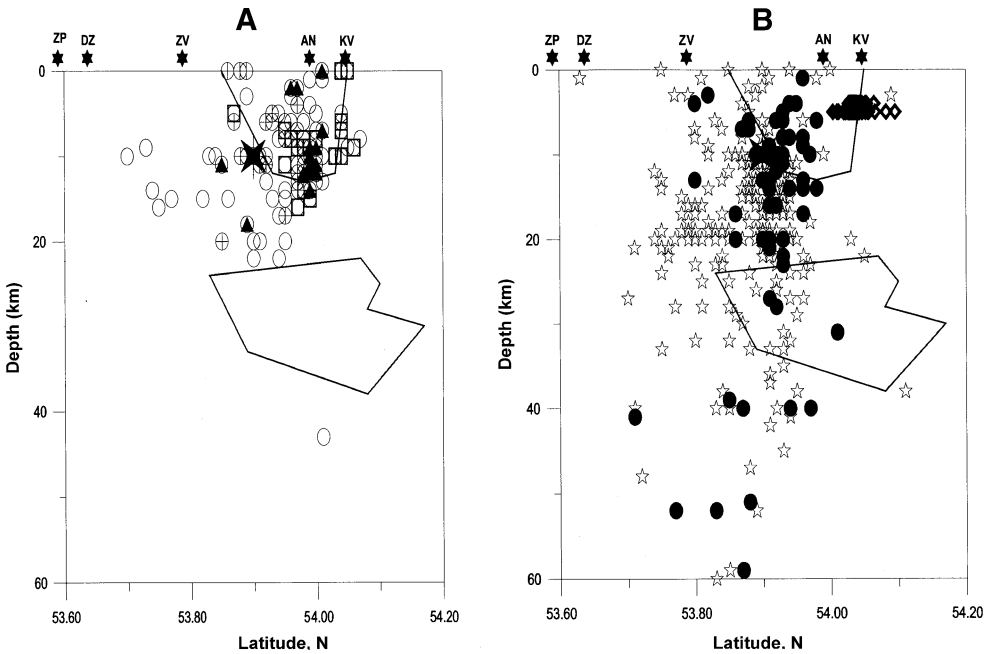

Fig. 14 Hypocenters of earthquakes (*mb*>2) located during 1972–1995 (**a**) and in January 1996 before the eruption in Karymskoye lake (**b**). The asperities that were destroyed during the *Mw* 7.1 earthquake are shown by *lines* (from Zobin and Levina 1998). All other *symbols* are the same as for Fig. 13. Data are from the Kamchatka Regional Earthquake Catalog

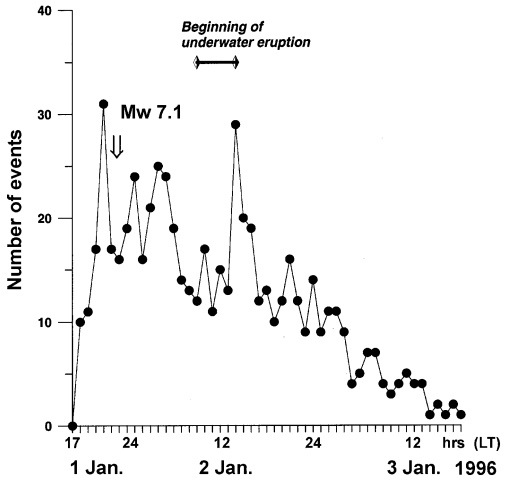

Fig. 15 Temporal variations of hourly earthquake numbers ($mb>2$) during the first 50 h of the January 1996 activity at Akademia Nauk volcano. Appearance of the *Mw* 7.1 earthquake is shown by the *arrow*. The probable time interval for the beginning of the eruption is noted. Data are from the Kamchatka Regional Earthquake Catalog

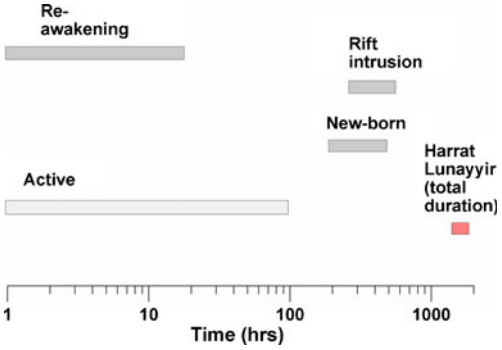

Fig. 16 Comparative durations of stage 2 for different types of basaltic eruptions and the total duration of the 2009 Harrat Lunayyir earthquake swarm

According to Table 1, it is possible to discuss the scenarios for future seismo-volcanic activity within Harrat Lunayyir and other lava fields covering an area of 180,000 km^2 within Saudi Arabia. All of them were formed during the past 30 Ma in response to Red Sea rifting (Pallister et al. 2010). In this sense, all these structures have the same potential of eruptive activity.

The 2009 episode at Harrat Lunayyir was characterized by the total duration of the seismic activity from 18 April to 27 June 2009, or about 1,700 h (Al-Amri and Al-Mogren 2011). This duration of the seismic activity was longer than any activity preceding the basaltic eruptions of different types (Table 1). Therefore, the most probable scenario is the arrest of sub-surface intrusion without any eruption in the region of Harrat Lunayyir.

At the same time, it is possible to consider this seismic swarm as preliminary, representing the stage 1. Then, the next probable scenario would be the process similar to the 2005–2009 dike injections along rift zones in Afar ("Seismic activity associated with dike injections along rift zones"). It is a structure very similar to the Saudi Arabian volcanic rifts and having preliminary seismo-tectonic crisis during 1978 and 1989 (Ayele et al. 2007). In this case, the 2009 episode would have a continuation of the seismic activity (stages 2 and 3) within Saudi Arabian Harraat adjacent to Harrat Lunayyir and accompanied by the surface dike intrusions.

Next probable scenario, having also the stage 1, may be re-awakening of the old Harrat Lunayyir volcano. This process, observed at Akademia Nauk volcano was characterized by three preliminary low-magnitude (up to *Ms* 5.5) and shallow earthquake swarms during 8 years before the volcano re-awakening. The appearance of new earthquake swarms within the Harrat Lunayyir lava field may be a signal of this type of scenario.

The birth of a new volcano at Harrat Lunayyir is less probable. This activity ("Seismic activity associated with new-born basaltic volcanoes") would be characterized by a 2–3-week earthquake swarm with the maximum magnitude earthquakes of about 5–5.5 and culminated by the birth of a new volcano. From this point, the 2009 swarm occurred already without appearance of new volcanic structure within Harrat Lunayyir lava field, and the process is over. At the same time, the birth of new volcanoes was observed during the 1256 Harrat Rahat eruption. Therefore, there is a probability of this process for other Harraat in Saudi Arabia.

Conclusions

Analysis of the seismic activity associated with different types of eruptions at basaltic volcanoes was carried out for the active, new-born, and re-awakening volcanic centers.

Table 1 Characteristic durations of three stages in seismic activity associated with basaltic eruptions

Type of eruption	Stage 1	Stage 2	Stage 3
Eruption at active volcano		0–120 h	
New-born volcano		300–500 h	2–3 months
Re-awakening volcano	Some years	20–30 h	
Rift intrusion	Some years	400–600 h	Some years

The obtained results were compared with the characteristics of the 2009 seismic crisis observed at the ancient Saudi Arabian lava fields Harrat Lunayyir. The duration of preceding stage of the seismic activity, defined as criteria of the type of volcanic crisis, varied from a few hours for active and re-awakened volcanoes to some weeks for newborn volcanoes. The duration of the seismic activity during the 2009 episode at Harrat Lunayyir was longer than any activity preceding the basaltic eruptions of different types. Therefore, the most probable scenario is the arrest of subsurface intrusion without any eruption in the region of Harrat Lunayyir. The next probable scenario would be the dike injections along the rift zones. The re-awakening of the old Harrat Lunayyir volcano or the birth of a new volcano at Harrat Lunayyir is less probable.

Acknowledgment The comments of two anonymous reviewers helped improve the manuscript. Catalogs of volcanic earthquakes were provided by Domenico Patané (Etna volcano, Italy), Jennifer Nakata (Kilauea volcano, Hawaii), and Valeria Levina (New Tolbachik volcanoes, Academia Nauk volcano).

References

Al-Amri AM, Al-Mogren SM (2011) Seismo-volcanic investigation of the current activity in Harrat Lunayyir, Al-Madinah Al-Munawwarah area. Final report. King Saud University, Riyadh, p 184

Allard P, Behncke B, D'Amico S, Neri M, Gambino S (2006) Mount Etna 1993–2005: anatomy of an evolving eruptive cycle. Earth-Sci Rev 78:85–114

Alparone S, Andronico D, Giammanco S, Lodato L (2004) A multidisciplinary approach to detect active pathways for magma migration and eruption at Mt. Etna (Sicily, Italy) before the 2001 and 2002–2003 eruptions. J Volcanol Geotherm Res 136:121–140

Ayele A, Jacques E, Kassim M, Kidane T, Omar A, Tait S, Nercessian A, de Chabalier J-B, King J (2007) The volcano-seismic crisis in Afar, Ethiopia, starting September 2005. Earth Planet Sci Lett 255:187–197

Ayele A, Keir D, Ebinger CJ, Wright TJ, Stuart GW, Buck R, Jacques E, Ogubazghi G, Sholan J (2009) The September 2005 mega-dike emplacement in the Ma-Hararo (Afar) nascent oceanic rift. Geophys Res Lett 36:L20306

Belousov A, Belousova M (2001) Eruptive process, effects deposits of the 1996 ancient basaltic phreatomagmatic eruptions in Karymskoe lake, Kamchatka, Russia. Spec Publs Int Ass Sediment 30:35–60

Chang S-J, Van der Lee S (2011) Mantle plumes and associated flow beneath Arabia East Africa. Earth Planet Sci Lett 302:448–454

Chen H, Gao F, Wu X, Meng X (2004) Relationship between earthquake and volcanic eruption inferred from historical records. Acta Seism Sin 17:500–506

Dziak RP, Fox CG, Schreiner AE (1995) The June–July 1993 seismo-acoustic event at CoAxial segment, Juan de Fuca Ridge: evidence for a lateral dike injection. Geophys Res Lett 22:135–138

Ebinger C, Ayele A, Keir D, Rowl JV, Yirgu G, Wright T, Belachew M, Hamling IJ (2010) Length and timescales of rift faulting magma intrusion: the Afar rifting cycle from 2005 to present. Annu Rev Earth Planet Sci 38:439–466

Fedotov SA (ed) (1984) Large Tolbachik fissure eruption. Nauka, Moscow, p 637 (in Russian)

Fedotov SA (1998) Study and mechanism of the simultaneous 1996 Karymsky volcano Akademia Nauk caldera eruptions in Kamchatka. Volc Seis 19:525–566

Harrigan P (2006) Volcanic Arabia Saudi. Aramco World 57:2–13

Klein FW, Koyanagi RY, Nakata JS, Tanigava WR (1987) The seismicity of Kilauea's magma system. US Geol Surv Prof Pap 1350:1019–1185

Luhr JF, Simkin T (eds) (1993) Parícutin. The volcano born in a Mexican cornfield. Geoscience Press Inc, Phoenix, p 427

Masurenkov YuP (1991) Tectonic position and general history evolution of Eastern Kamchatka volcanoes. In: SA Fedotov, YuP Masurenkov (eds) Active volcanoes of Kamchatka, Vol 2, Nauka, Moscow, pp 8–15 (In Russian)

Matsumura S, Ohkubo T, Imoto M (1991) Seismic swarm activity in and around the Izu Peninsula preceding the volcanic eruption of July 13, 1989. J Phys Earth 39:93–106

Pallister JS, McCausl WA, Jónsson S, Lu ZHM, El Hadidy S, Aburukbah A, Stewart ICF, Lundgren PR, White RA, Moufti MRH (2010) Broad accommodation of rift-related extension recorded by dyke intrusion in Saudi Arabia. Nature Geosciences 3:705–712

Patanè D, Privitera E, Gresta S, Akinci A, Alparone S, Barberi G, Chiaraluce L, Cocina O, D'Amico S, De Gori P, Di Grazia G, Falsaperla S, Ferrari F, Gambino S, Giampiccolo E, Langer H, Maiolino V, Moretti M, Mostaccio A, Musumeci C, Piccinini D, Reitano D, Scarfì L, Spampinato S, Ursino A, Zuccarello A (2003) Seismological constraints for the dike emplacement of July–August 2001 lateral eruption at Mt Etna volcano, Italy. Ann Geoph 46:599–608

Spera FJ (2000) Physical properties of magma. In: Sigurdsson H (ed) Encyclopedia of volcanoes. Academic, San Diego, pp 171–190

Vergniolle S, Mangan M (2000) Hawaiian and Strombolian eruptions. In: Sigurdsson H (ed) Encyclopedia of volcanoes. Academic, San Diego, pp 447–461

Yamasato H, Yokota T, Kashiwabara S (1991) Earthquake swarm volcanic tremors off Eastern Izu Peninsula in 1989. Spectral investigation and characteristics of waveforms. J Phys Earth 39:79–92

Zobin VM (2003) Introduction to volcanic seismology. Elsevier, Amsterdam, p 304

Zobin VM, Gorelchik VI (1982) Seismicity source parameters of earthquakes in the region of the Large Tolbachik fissure eruption. Bull Volcanol 45:99–113

Zobin VM, Firstov PP, Ivanova EI (1983) Earthquake swarm in the region of Karymsky Volcano in Jan.–Feb., 1978. Volcanol Seismol 5:64–73, In Russian

Zobin VM, Levina VI (1998) Rupture history of the 1996 January 1 Ms 66 volcanic earthquake preceding the simultaneous eruption of Karymsky Akademia Nauk volcanoes in Kamchatka, Russia. J Geophys Res 103:18315–18324

WEB sites

BGVN (2005) Bulletin of the Global Volcano Network, Smithsonian Institution, Washington. http://www.volcano.si.edu/reports/bulletin/ Last visit on 1 June 2011

GVP (2011) Global Volcano Project, Smithsonian Institution, Washington. http://www.volcano.si.edu/ Last visit on 1 June 2011

Harvard CMT (2011) Centroid moment tensor (CMT) catalog, Harvard University, Harvard. http://www.globalcmt.org/CMTsearch.html. Last visit on 1 June 2011

ISC (2011) Bulletin of the International Seismological Centre, Thatcham. http://www.isc.ac.uk/doc/products/bulletin.html Last visit on 1 June 2011

USGS. (2011) US Geological Survey Earthquake Hazards Program, Reston. http://earthquake.usgs.gov/earthquakes/eqarchives/epic/ Last visit on 1 June 2011